Opto-Electronic Advances
光电进展

Mid-infrared all-fiber gain-switched pulsed laser at 3 μm

Xiaojin Zhang, Weiwei Li, Jin Li, Huiying Xu, Zhiping Cai and Zhengqian Luo*

http://dx.doi.org/10.29026/oea.2020.190032

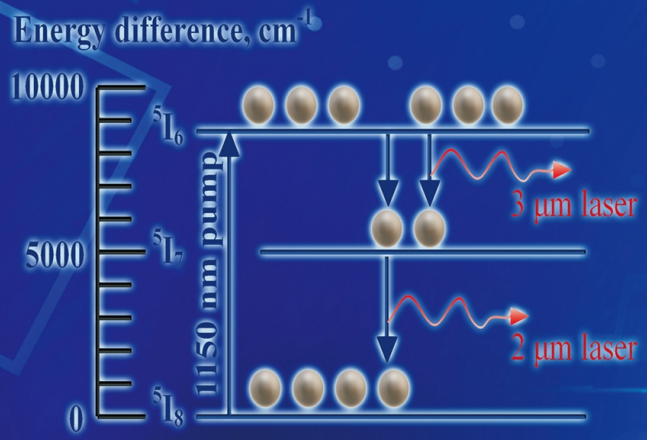

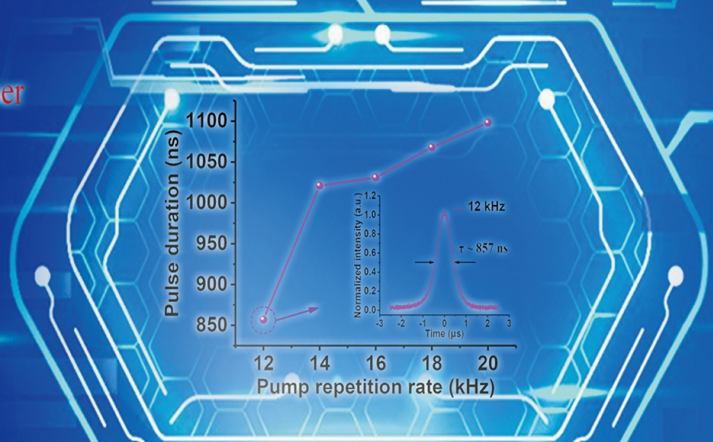

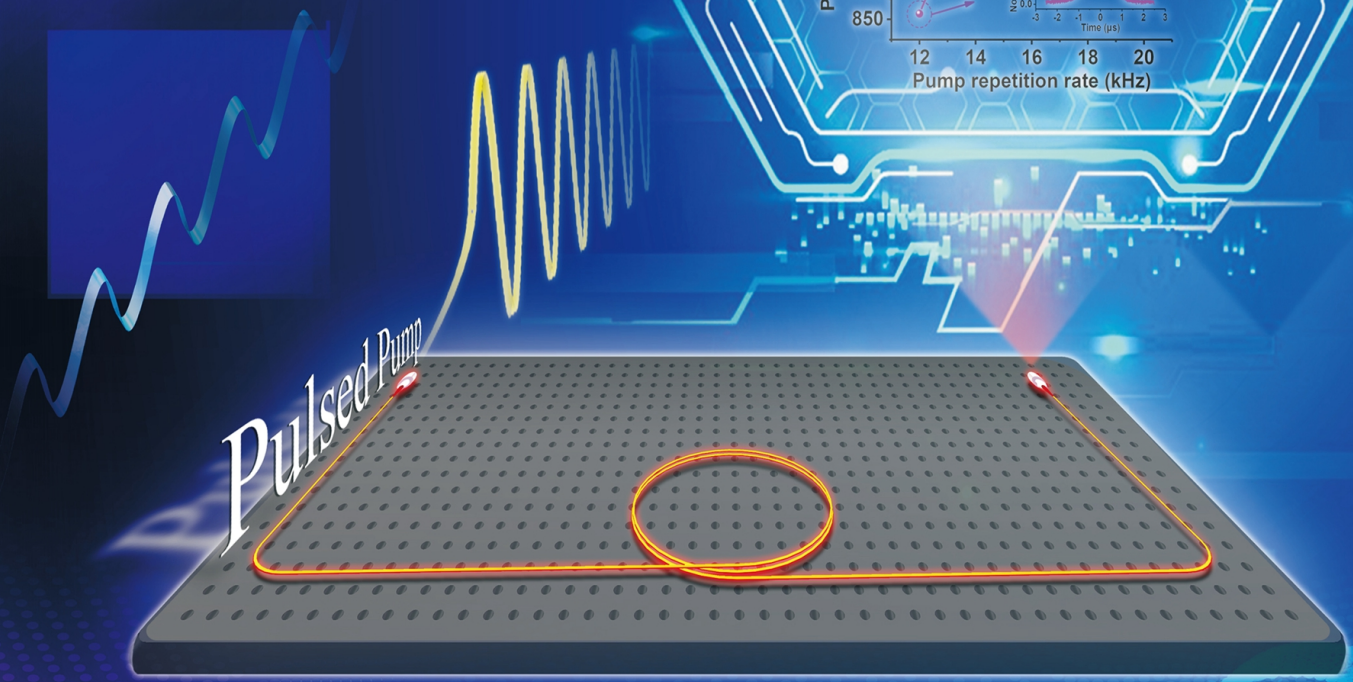

Opto-Electronic Advances

Original Article

2020, Vol. 3, No. 5

DOI: 10.29026/oea.2020.190032

Mid-infrared all-fiber gain-switched pulsed laser at 3 μm

Xiaojin Zhang, Weiwei Li, Jin Li, Huiying Xu, Zhiping Cai and Zhengqian Luo*

Mid-infrared (MIR) fiber pulsed lasers are of tremendous application interest in eye-safe LIDAR, spectroscopy, chemical detection and medicine. So far, these MIR lasers largely required bulk optical elements, complex free-space light alignment and large footprint, precluding compact all-fiber structure. Here, we proposed and demonstrated an all-fiberized structured gain-switched Ho^{3+}-doped ZBLAN fiber laser operating around 2.9 μm. A home-made 1146 nm Raman fiber pulsed laser was utilized to pump highly concentrated single-cladding Ho^{3+}-doped ZBLAN fiber with different lengths of 2 m or 0.25 m. A home-made MIR fiber mirror and a perpendicular-polished ZBLAN fiber end construct the all-fiberized MIR cavity. Stable gain-switched multiple states with a sub-pulse number tuned from 1 to 8 were observed. The effects of gain fiber length, pump power, pump repetition rate and output coupling ratio on performance of gain-switched pulses were further investigated in detail. The shortest pulse duration of 283 ns was attained with 10 kHz repetition rate. The pulsed laser, centered at 2.92 μm, had a maximum average output power of 54.2 mW and a slope efficiency of 10.12%. It is, to the best of our knowledge, the first time to demonstrate a mid-infrared gain-switched Ho^{3+}:ZBLAN fiber laser with compact all-fiber structure.

Keywords: fiber laser; mid-infrared; gain-switching

Zhang X J, Li W W, Li J, Xu H Y, Cai Z P et al. Mid-infrared all-fiber gain-switched pulsed laser at 3 μm. *Opto-Electron Adv* **3**, 190032 (2020).

Introduction

On account of abroad applications in remote sensing[1], scientific research, medical surgery[2] and electro-optical countermeasure[3], mid-infrared (MIR) lasers have attracted increased interest. In particular, laser sources emitting at ~3 μm waveband, which overlaps with the absorption peaks of water molecules, can be served as a secure laser scalpel in laser surgery. Over the past few years, MIR fluoride fiber lasers doped with rare earth elements (e.g. Er^{3+} [4–6], Ho^{3+} [7–9], Dy^{3+}[10,11], etc.) have got extensive attention due to their inherent merits of compactness, good system stability, reduced thermal effects, low operating cost, and excellent beam quality. Mid-infrared pulsed fiber lasers, which can provide high peak power, and high energy, have special application prospects compared with continuous-wave (CW) laser sources, such as material processing and optical communication, and some applications in which they cannot be replaced. Q-switching and gain-switching are two well-known methods to generate ns- or μs-order pulsed laser output. Usually, Q-switched fiber lasers operating around 3 μm are obtained by modulating the Q-factor of the laser cavity actively with modulators such as mechanical shutter[12], acousto-optic modulator (AOM)[13], and passively with saturable absorbers (SAs) such as semiconductor saturable mirror (SESAM)[8,14], InAs epilayers[15], Fe^{2+}:ZnSe crystal[16], 2D materials[17–19], 3D topological Dirac semimetal material[20], etc.

It is well-known that Q-switching technique inevitably requires to insert bulk modulator or SAs into fiber laser cavity, which reduces the robustness and compactness of

Department of Electronic Engineering, Xiamen University, Xiamen 361005, China.
*Correspondence: Z Q Luo, E-mail: zqluo@xmu.edu.cn
Received: 4 August 2019; Accepted: 24 September 2019; Published: 21 May 2020

laser system. In contrast, gain-switched laser pulses are achieved by way of switching the gain of laser cavity without any additional cavity modulators, thereby making the structure more compact, lower costs, and reducing intracavity loss. Thus, a variety of gain-switched fiber lasers emitting in MIR regime have been reported[21–32]. In 2001, Dickinson et al. firstly demonstrated a Er^{3+}/Pr^{3+}-codoped ZBLAN fiber laser pumped by 791 nm pump source, with a pulse energy of 1.9 mJ, a slope efficiency of 13.5% and a center wavelength of 2.7 μm[21]. Subsequently, Gorjan et al. reported a gain-switched Er^{3+}-doped fluoride fiber laser through the use of active pulsed diode pumping, and 68 W peak power with 100 kHz repetition rate was obtained[23]. In 2015, Shen et al. developed a MIR pulsed Er^{3+}-doped fluoride fiber laser operating in fundamental-transverse-mode with a pulse duration of 1.18 μs at a repetition rate of 10 kHz, reaching highest pulse energy of 4.2 μJ[22]. Recently, a few works on gain-switched holmium doped fluoride fiber lasers have been done[24,25,27,31]. In 2017, via the cascaded gain-switching technology, Luo et al. represented a double wavelength pulsed Ho^{3+}:ZBLAN fiber laser around 3 μm and 2 μm, and gain-switching pulses at ~3 μm were achieved with a narrowest pulse duration of 0.824 μs and output power of 262.14 mW[27]. Very recently, they also demonstrated a gain-switched wavelength-tunable fiber laser by adopting a planar grating, and the widely tunable range of 105 nm from 2895.5 nm to 3000.5 nm was successfully obtained[25]. However, almost all of mid-infrared gain-switched fiber lasers require bulk optical components to construct MIR laser system, precluding a compact all-fiber structure. There are two main challenges for MIR all-fiber cavity. First, the lack of fiber-compatible MIR mirror restricts the formation of MIR all-fiber cavity, resulting in the use of complex free-spacing alignments (e.g. a lot of coupling lens). Second, fluoride fibers are difficult to fuse splicing with other fibers.

In this article, a demonstration of gain-switched Ho^{3+}:ZBLAN all-fiberized laser operating at ~2.9 μm was given. In our experimental apparatus, a home-made 1146 nm Raman fiber pulsed laser was used for pumping a highly concentrated single-cladding Ho^{3+}-doped zirconium fluoride fiber with different lengths of 2 m and 0.25 m. The MIR end-facet mirrors were utilized to form the all-fiber MIR cavity. The effects of the gain fiber length, pump average power, pump repetition rate on the build-up time and duration of gain-switched pulse were discussed. Moreover, several influence of output coupling on the pulse width and output wavelength of gain-switched fiber laser was studied as well. Stabilized and reliable gain-switched multiple pulse trains were obtained from both cavities with the repetition rate of 20 kHz, while two kinds of stable temporal states (i.e. "1-1" and "2-1" state) were observed from the 2 m long fiber laser.

Experimental set-up

The schematic diagram of our proposed 3 μm gain-switched Ho^{3+}:ZBLAN fiber laser is illustrated in Fig. 1. The gain-switched laser with all-fiber structures is mainly composed by the 1146 nm laser pumping source, resonant cavity, and Ho^{3+}-doped ZBLAN fiber. The pump source is a homemade 1146 nm Raman pulsed fiber laser, whose repetition rate can be tuned from 10 kHz to 20 kHz. With the purpose of increasing absorption ratio of pumping laser pulse energy, two pieces of single-clad Ho^{3+}-doped fibers (Le Verre Flouré Inc.) available for single mode transmission at ~3 μm waveband with different lengths of 0.25 m and 2 m are used as gain mediums to be contrasted. The numerical aperture of the gain fiber is 0.23 with core/cladding diameters of 7.5/125 μm. Besides, its doping concentration is determined as high as

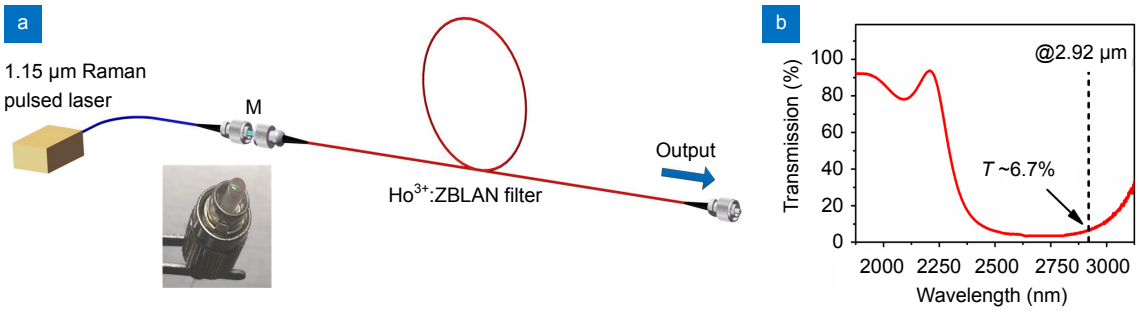

Fig. 1 | (**a**) The experiment device diagram of the compact 3 μm gain-switched laser with an all-fiberized structure. Inset: actual photo of the fiber end-facet mirror M. (b) Measured transmission optical spectrum of the M.

5000 ppm, which provides a high pump absorption coefficient of ~40 dB/m. The all-fiber linear resonant cavity is comprised of a home-made fiber end-facet mirror (M) utilized as input coupler and the 4% Fresnel reflection of the polished gain fiber face used for output coupling. The fiber end-facet mirror used to reflect laser signal was manufactured by sputter coating technology utilizing a plasma sputter deposition system. As displayed in the inset photo of Fig. 1(a), the reflector M was directly plated on the whole end face of the silicate single-mode fiber. Figure 1(b) depicts the measured transmission spectrum of mirror M, which shows a lower transmission of <10%, corresponding to a higher reflectivity of >90% in the 2500–3000 nm waveband. A ceramic sleeve, which was applied to provide high coupling efficiency between the Ho^{3+}-doped ZBLAN fiber and other fibers (e.g. the conventional silicate SMF) in our experiment in order to obtain an all-fiber structure, has an inner diameter of 2.5 mm. Such setup had a measured high coupling efficiency of ~80%. The radio-frequency (RF) spectra and output optical spectra were measured by means of an electrical spectrum analyzer and an optical spectrum analyzer. An 100 MHz oscilloscope was applied to synchronously monitor the waveforms of the pump pulse and laser pulse output.

Results and discussion

Pulse evolution as pump power

In our experiment, we studied the establishment of the output ~3 μm gain-switching pulses from the 2 m and 0.25 m long fibers with increasing pump power at 1146 nm. Firstly, the repetition rate of the 1.15 μm pump source was fixed at a value of 20 kHz. It should be pointed out that the pump pulse duration in this part of experiment vary from 35 μs to 45 μs, while the lifetime of the high energy level $^5I_6$ in Ho^{3+}-doped zirconium fluoride fiber measured as ~3.5 ms[33] is relatively long, so that stabilized gain-switch pulses can be generated. For the 2 m long laser cavity, with the incident pump power reached 52 mW, gain-switching pulses could be observed but unstable and fluctuant. It should be noted that the pump power referred to in this letter are defined as average power if not specially stated. When the pump power continued to be increased, steady gain-switching pulse trains were obtained at the repetition rate of 20 kHz in accordance with pump. The time domain characteristics of the stable gain-switching pulse trains output from 3 μm fiber laser were shown in Fig. 2(a). As the pump power was set to ≤79 mW, the stable single pulse operation could be maintained. Once over this value of pump power, stable multi-pulse trains were generated, the number of sub-pulse could be continually switched from 1 to 8 through adjusting the pump power from 100 mW to 597 mW, and the intensities of sub-pulse decreased gradually. Such a phenomenon of multiple pulse has been already observed in previous reports of Er^{3+}-doped ZBLAN fiber laser[22,30] and Tm^{3+}-doped fiber laser[34–35]. This can be explained as follows. Once the pump pulse energy is too high, after producing the first laser pulse, the particles of upper energy level $^5I_6$ will repopulate by absorbing the residual pump energy and then release energy again, thus a second laser pulse or even more sub-pulses appeared. Emphasized that there exits chaotic time domain characteristics between different stable states as a result of

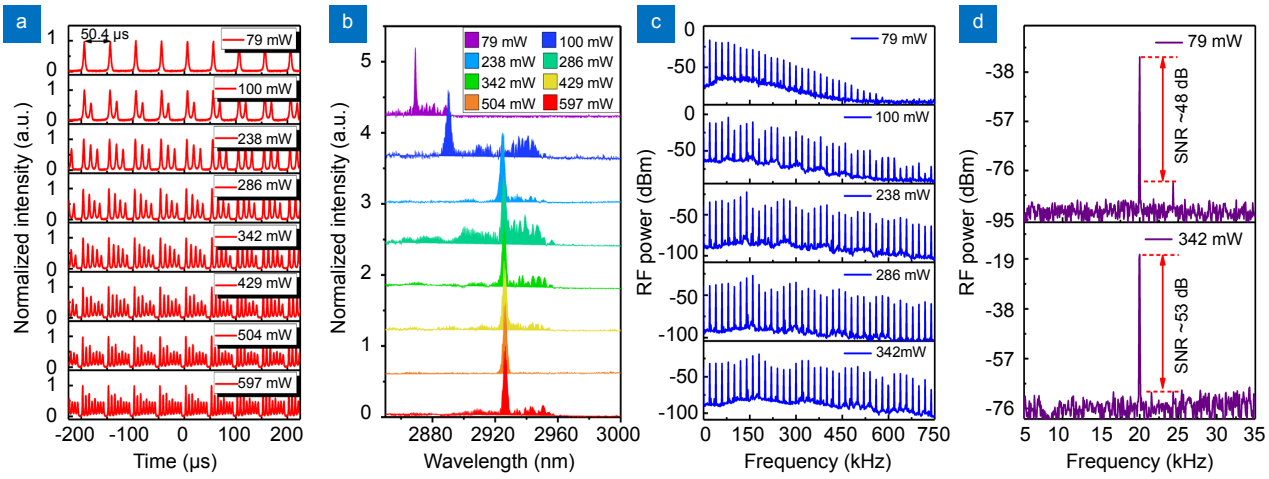

Fig. 2 | Under various pump powers and a fixed 20 kHz repetition rate, measured (a) stable gain-switched multi-pulse trains, (b) typical output optical spectra, (c) broadband RF output spectra, and (d) RF spectra at the fundamental frequency peak from the 2 m long fiber laser.

mode-hopping and mode competition[36]. Stabilized multi-pulse trains couldn't be captured showing unstable relaxation spike pulses once the pump power raised higher than 597 mW.

Figure 2(b) gives the optical spectra of our 3 μm gain-switched Ho^{3+}:ZBLAN fiber laser at several kinds of temporal states from 2 m long gain fiber. As the pump power increasing from 79 mW to 597 mW, central wavelength red shifted from 2869.1 nm to 2926.5 nm for the reason of reabsorption effect. The output RF spectrum characteristics of stable gain-switched multi-pulses in a wide range of 750 kHz with different sub-pulse number from 1 to 5 were shown in Fig. 2(c). One can see that the modulations of RF spectrum intensity in multi-pulse states are distinctly different from the single-pulse state, which accord with Fourier transform of multiple sub-pulses. As plotted in Fig. 2(d), the fundamental frequency of laser pulse was located at 20 kHz. The RF signal-to-noise (SNR) was over 45 dB when pump power was 79 mW , and increased to >50 dB with pump power reached 342 mW, indicating the good stability of our gain-switched laser system. The effect of pump energy on multi-pulse set-up time was investigated by simultaneously monitoring the pulsed pump and laser signal, and the results are depicted in Fig. 3. As can be intuitively observed from these diagrams, the pulse build-up time shortened from 28.44 μs to 4.84 μs with increased pump power due to accelerating the population inversion under higher pumping energy.

Similar phenomenon was observed from the 0.25 m long gain-switched fiber laser while pump repetition rate was set as 20 kHz. The results are given in Fig. 4. It serves to show from Fig. 4(a) that stable single-pulse operation was obtained at the pump power of 80 mW, and stable multi-pulse gain-switching with a number of sub-pulse varied between two and eight pulses occurred under the pump power increased from 102 mW to 679 mW, respectively. As shown in Fig. 4(b), the RF spectrum modulation corresponding to multiple sub-pulses was observed as well. Figure 4(c) illustrated the output optical spectrum from the gain-switched laser when the average pump power arrived at 80 mW and 697 mW, showing a wavelength centered at ~2865 nm with a slight red-shift. Compared with the red-shift wavelength in 2 m long cavity, it indicated that the reabsorption effect of the long fiber is stronger than the shorter one, which may offer a widely tunable laser.

In addition, as plotted in Fig. 4(d), the output average power from the 2 m long fiber laser compared with that of 0.25 m long fiber lasers was further analyzed. A maximum ~3 μm output average power of 54.2 mW was obtained from 2 m long fiber under 597 mW pump power. The slope efficiency of the 2 m long fiber laser was identified as 10.12%, and a low slope efficiency of 0.71% for the 0.25 m long fiber laser. The slope efficiency enhanced with the fiber length increasing, which could be explained by the possibility that more pump energy was absorbed by longer fiber than the shorter one to acquire more gain.

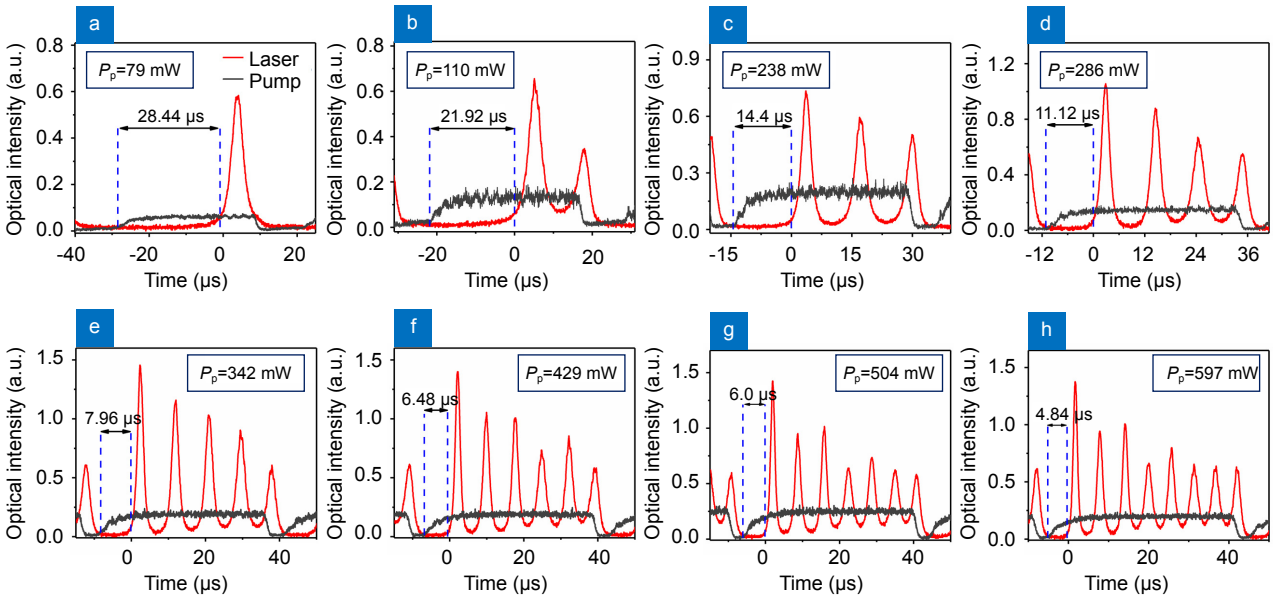

Fig. 3 | Temporal pump and gain-switched multi-pulses in one period produced by 2 m long fiber laser under different pump powers of (a) 79 mW, (b) 100 mW, (c) 238 mW, (d) 286 mW, (e) 342 mW, (f) 429 mW, (g) 504 mW, (h) 597 mW.

Single-pulse operation under different repetition rates

From above experiment, we were consciously aware that pump power (pump energy) have important impact on the performance above all the establishing of multi-pulse of gain-switched fiber laser. In a follow-up work, we made an investigation into the influence of pump repetition rate on single-pulse evolution from 2 m and 0.25 m long cavities. The pump repetition rate of our home-made pump laser could be adjusted from 10 kHz to 20 kHz. In order to realize single-pulse operation at varying pump repetition rates, the pump power would be adjusted within a certain value to avoid generating multi-pulse and the pump duration was set to a minimum value of ~11 μs in our pump laser system.

With the pump pulse duration set to ~11 μs, stable gain-switched single-pulse trains at varied pump repetition rates were attained from 2 m long and 0.25 m long fiber laser. The single-pulse trains generated from a 2 m long fiber were plotted in Figs. 5(a) and 5(b). For the 2 m long fiber laser, when the pump repetition rate was switched to a low value of 10 kHz, no stabilized single-pulse trains could be gained. The first observation was that only stable "1-1" state (i.e. every one pump pulse produced one gain-switched pulse) was obtained on increasing the pump repetition rate from 12 kHz to 16 kHz.

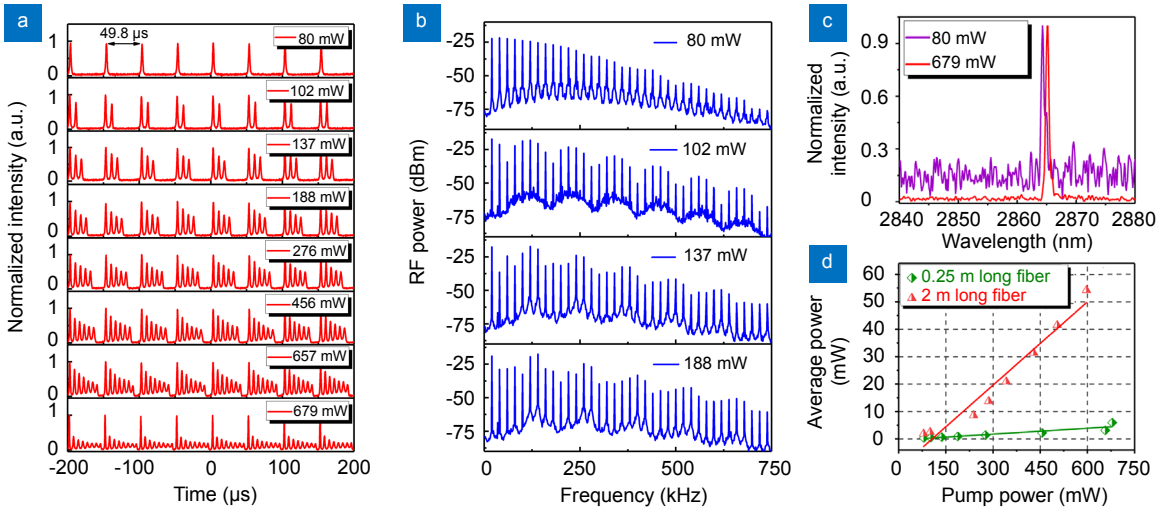

Fig. 4 | Measured (**a**) stable gain-switched multi-pulse trains and (**b**) broadband RF output spectrums. (**c**) Optical spectrums at a 20 kHz pump repetition rate from the 0.25 m long fiber laser. (**d**) The relationships between average output power and pump power of two kinds of cavities.

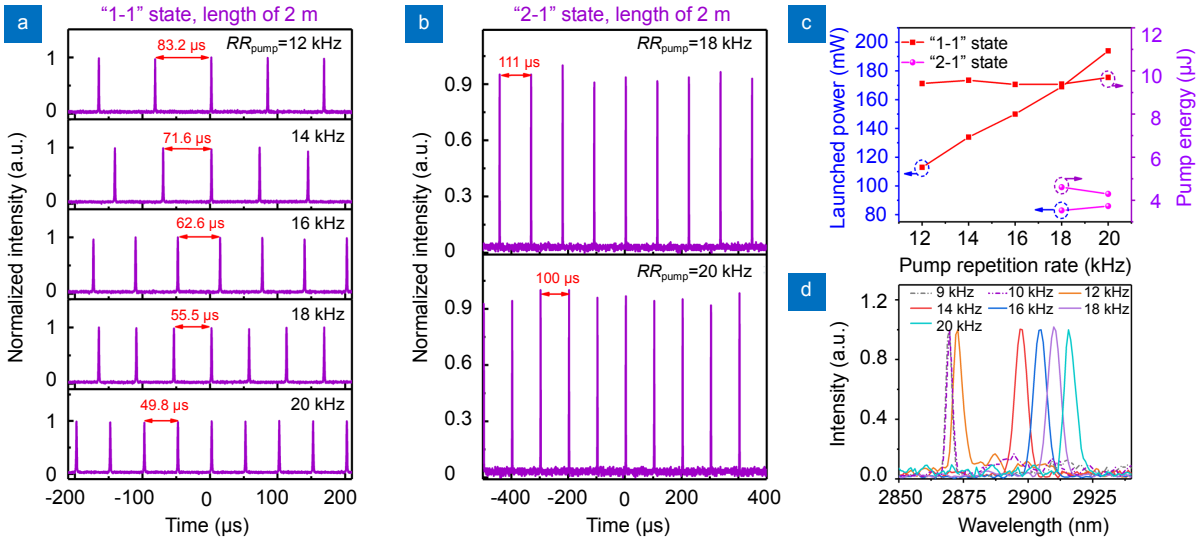

Fig. 5 | Output characteristics from the 2 m long cavity. Stable gain-switched single-pulse trains at (**a**) "1-1" state and (**b**) "2-1" state was generated with increased pump repetition rate. (**c**) The required pump power and pulse energy threshold varied with the pump repetition rate at different temporal states, respectively. (**d**) Output optical spectrums at different laser repetition rates, where dash lines represent "2-1" state and solid lines represent "1-1" state.

As the repetition rate increased to ≥18 kHz, stable "1-1" and "2-1"(i.e. every two pump pulses produced one gain-switching pulse) states would be obtained. The results indicate that the higher the pump repetition rate, the more kinds of stable single-pulse states can be observed, which are well comparable to the results obtained in previous reports[25,29]. The time intervals decreased from 111 μs to 49.8 μs corresponding to the laser pulse repetition rate range of 9 kHz to 20 kHz with slightly fluctuating amplitudes. The comparison of pumping power and pulse energy threshold required in two states at various pump repetition rates was given, as shown in Fig. 5(c). At the lower pump powers (pump energy) of 83 mW (4.6 μJ) and 86 mW (4.3 μJ), generating "2-1" state suggested that energy of one pump pulse is insufficient to reach the threshold of population inversion. Moreover, it is interesting to note that, the pump energy of the 2 m long fiber laser at "1-1" state slightly floated up and down between 9.41 μJ and 9.70 μJ, which was different from the results in the 0.25 m long fiber laser, and the reasons will be analyzed in detail in the following. The output optical spectrums at two stable states with varying laser repetition rates were plotted in Fig. 5(d). It can be found that the wavelength in "1-1" state shifted toward long wavelength quickly from 2872.8 nm to 2897.7 nm and then shifted slowly to 2915.6 nm, but kept unchanged at about 2869 nm in "2-1" state, under increasing pump repetition rate from 12 kHz to 20 kHz.

Figure 6 indicates the output characteristics from the 0.25 m long fiber laser. Different from the output state of 2 m long cavity, "1-1" state always existed between 10 kHz and 20 kHz pump repetition rate, as can be seen in Fig. 6(a). Whereas, there was no "2-1" state observed during the whole process. The measured pump power thresholds and pump pulse energies under varied pump repetition rates from 10 kHz to 20 kHz were shown in Fig. 6(b). One can see that the pump energy threshold of 0.25 m long gain-switched fiber laser was decreased monotonically from 9.5 μJ to 6.25 μJ with increased pump power threshold from 95 mW to 125 mW. This finding can be interpreted that with the increase of pump repetition rate, corresponding pumping cycle becomes shorter, which lead to more populations remaining in the upper laser level $^5I_6$ in one pump period, thus lower the pump energy threshold. Equally, we monitored its center wavelength changes of output spectrum. It is identified that the wavelength remained invariant wavelength of ~2865 nm, which can be seen in Fig. 6(c). Comparing two different results of 2 m and 0.25 m long fiber laser, the fluctuation of pump pulse energy threshold displayed in Fig. 5(c) from 2 m long cavity was likely due to the wavelength drifting according to Ref.[25], and more populations remained in the energy level $^5I_7$ since the terminated Stark level was up-shifted along with red-shift of wavelength, leading to more populations in upper level $^5I_6$ required to reach inversion threshold.

Presented in Fig. 7 are the measured laser pulse durations, output average power, calculated pulse energy and peak power at "1-1" state from 2 m and 0.25 m long fiber laser versus the pump repetition rate. For 2 m long cavity,

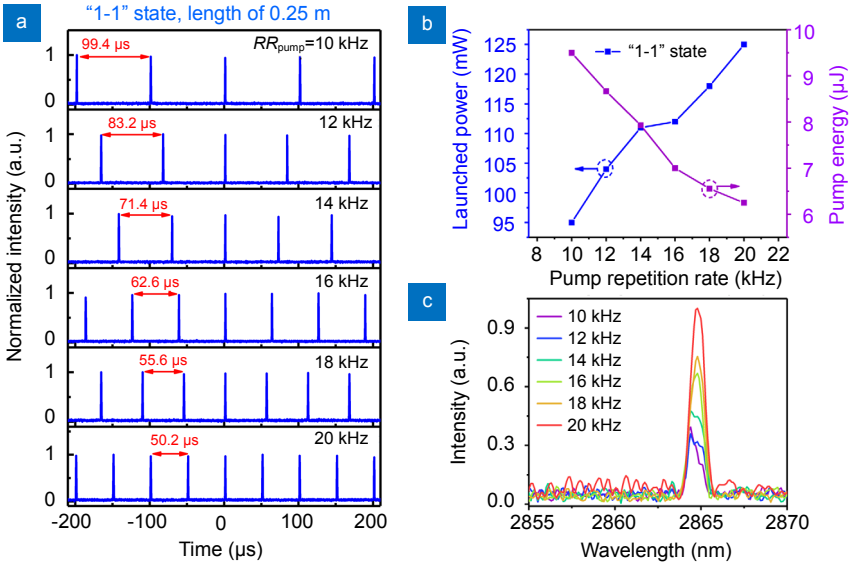

Fig. 6 | Performance characteristics from the 0.25 m long cavity. (**a**) With increasing pump repetition rate, stable gain-switched single-pulse trains were generated at "1-1" state. (**b**) Measured pump power threshold and calculated pump pulse energy under various pump repetition rate at "1-1" state, respectively. (**c**) Output optical spectrums at different laser repetition rates.

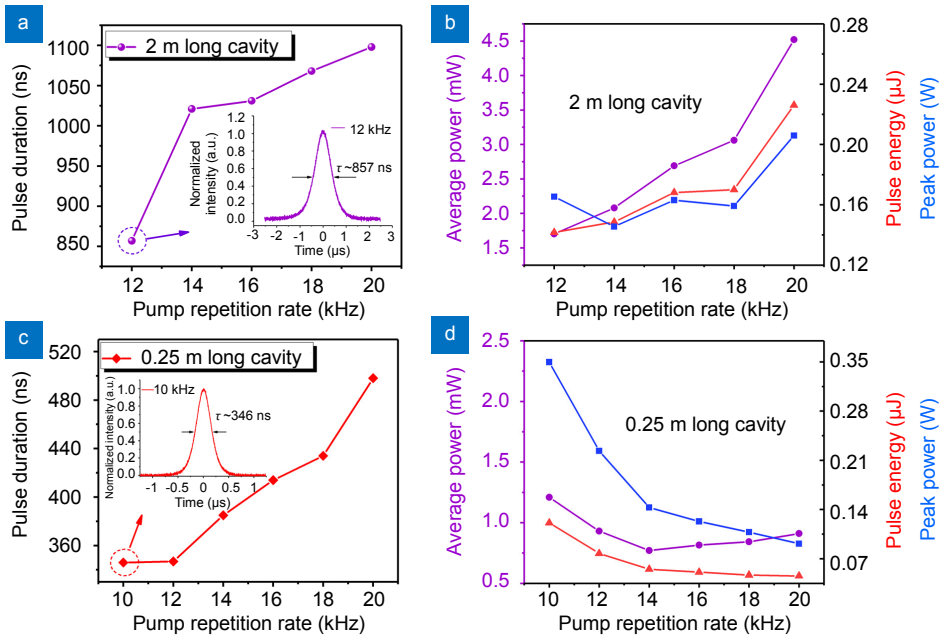

Fig. 7 | Output characteristics obtained from 2 m and 0.25 m long cavities, respectively. Both (**a**) and (**c**) are pulse durations, (**b**) and (**d**) are average output powers, single pulse energies, peak powers measured with different pump repetition rates, Inset: single pulse waveform in one period.

the pulse duration increased rapidly from 857 ns to 1021 ns and then became slowly up to 1098 ns with the increasing pump repetition rate, and in terms of shorter one, it continuously increased from 346 ns to 498 ns, as plotted in Figs. 7(a) and 7(c), respectively. On one hand, the pulse duration had positive correlation with repetition rate owing to less populations accumulating on the upper level $^5I_6$ after each pump pulse with the increased pump repetition rate and decreased pump pulse energy. On the other hand, the output pulse duration was shortened by the shorter gain fiber, which is matched with the results in Ref.[37]. Figs. 7(b) and 7(d) show the performance parameters of output power, pulse energy, and peak power of the long cavity and other short ones. It is noted that the output average power in 2 m cavity increased with pump repetition rate, exhibiting a linear trend in the measured repetition rate range. Corresponding output pulse energy increased from 140 nJ to 226 nJ. When pump repetition rate increased up to 20 kHz, a maximum peak power of 0.2 W was achieved. On contrary, output power varied non-monotonous was given from the 0.25 m long fiber laser, which showed a less change due to the limited absorption of short fiber. Decreasing pulse energy from 121 nJ to 45 nJ under the increasing pump repetition rate results from very slightly changed output power with a increased pulse repetition rate.

From what has been mentioned above, we may find that longer cavity is likely to obtain more gain switching temporal states under various pump repetition rate than short cavity based on Ho^{3+}-doped ZBLAN fiber laser. In addition, a shorter resonator cavity and a lower pump repetition rate may contribute to a shorter pulse width.

Influence of output coupling on single-pulse laser performance

To study the influence of output coupling on the performance of gain-switching Ho^{3+}-doped ZBLAN all-fiberized laser including gain-switching temporal state, pulse width, and wavelength, a high reflection output mirror was utilized to make a high-reflection (HR) cavity. The output mirror M2 coated on the end-facet of undoped zirconium fluoride fiber (Fiberlabs Inc.) had a consistent transmission spectrum with the input mirror M, showing a highly reflecting (>90%) at the laser waveband. The following results were compared with those of low-reflection (LR) cavity which utilized 4% Fresnel reflection as an output coupler.

Firstly, we investigated the change of temporal state from the 2 m and 0.25 m fiber laser equipped with the output coupler. It was found in surprise that in the 2 m long HR cavity, stable “1-1” state could only be observed when the pump repetition rate was switched to the maximum value of 20 kHz, yet, “2-1” state was always attained with the decrease of pump repetition rate from 20 to 16

kHz. Less temporal states were generated from 2 m fiber laser, but the 0.25 m fiber laser could still produce different temporal states as the pump repetition rate varied from 10 kHz to 20 kHz, comparing with the LR cavity. The causes are not clear, and need to be further studied.

Subsequently, the variations of pulse duration from both cavity configurations at the same pump repetition rate were also made a comparison. Figures 8(a) and 8(b) were the monitored single pulse waveforms plotted in stable "2-1" state from 2 m cavity, 8(c) and 8(d) were plotted in "1-1" state from 0.25 m cavity, respectively. As can be seen, the pulse duration generated with an output mirror was shorter than that without the mirror. It suggested that higher output coupling ratio may lead to shorter pulse duration. The pulse duration was decreased with the decreasing pump repetition rate, which has been mentioned in the second part, therefore the pulses with a shortest duration of 283 ns (see Fig. 8(d)) was achieved from the 0.25 m long HR cavity configuration, and its corresponding pulse repetition rate and output average power were 10 kHz and 330 μW, respectively.

Finally, the output spectrum of different laser cavity configurations was received, as displayed in Fig. 9. When the average power and repetition rate of pump source were switched to 110 mW and 20 kHz, respectively, the center wavelength of the 2 m fiber laser without output mirror was measured as ~2890 nm, and the another one with the mirror is about 2930.4 nm. The similar results were also found from the 0.25 m fiber laser under 670 mW pump power. The center wavelength exhibits obvious red-shift as a result of enhanced reabsorption with increased photon density in the cavity.

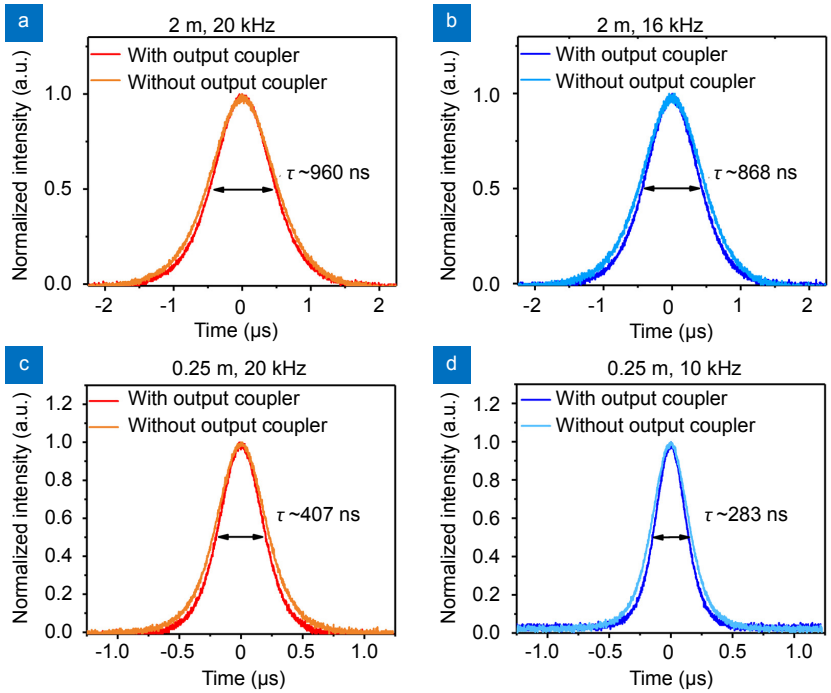

Fig. 8 | Output single pulse waveforms with or without the output coupler for different fiber lengths and repetition rates of (a) 2 m, 20 kHz, (b) 2 m, 16 kHz, (c) 0.25 m, 20 kHz, (d) 0.25 m, 10 kHz.

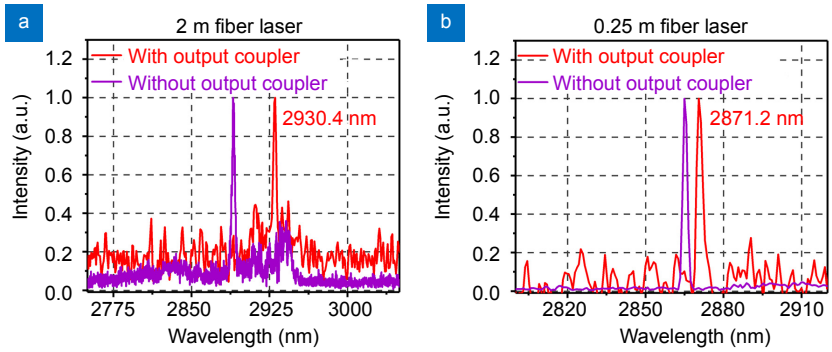

Fig. 9 | Optical spectrums measured from the MIR gain-switched laser for different fiber lengths and pump powers of (a) 2 m, 110 mW, (b) 0.25 m, 670 mW, under 20 kHz pump repetition rate.

Conclusions

In short, a compact gain-switched Ho^{3+}:ZBLAN all-fiber laser operating around 2.9 μm which locates in the water vapor absorption peak has developed successfully. A home-made Raman pulsed laser was used to pump the single-cladding Ho^{3+}-doped ZBLAN fiber which made sure of a transverse-single-mode laser output. Stable gain-switching multi-pulse trains were achieved with repetition rate of 20 kHz from two cavities configurations using the 2 m long gain fiber and 0.25 m long fiber. The multi-pulse laser can find significant applications in scientific researched, laser perforating, and communication domain. Besides, a laser with the stabilized single-pulse output was generated with a repetition rate limited by our pump source from 9 kHz to 20 kHz. Laser output wavelength switched from 2869 nm to 2915.6 nm was observed from the long fiber multi-pulse laser due to stronger reabsorption from the Stark level $^6I_5$. With the pump pulse width fixed to a minimum value of ~11 μs, the shortest pulse width attained is 283 ns at 10 kHz repetition rate from the high-reflection cavity. Furthermore, the experimental results show that when the laser is set at single-pulse gain-switching operation, the low pump repetition rate could help to get a narrower pulse duration, but the high repetition rate pumping could observe more temporal states. Further, performance improvements of our all-fiberized laser should be considered, and adopting a master oscillator power amplifier system to amplify output power will be a viable option.

References

1. Arnold G E, Hiesinger H, Helbert J, Peter G, Walter I. MERTIS−thermal infrared imaging of Mercury: advances in mid-IR remote sensing technology for planetary exploration. *Proc SPIE* **7808**, 78080I (2010).
2. Kaufmann R, Hartmann A, Hibst R. Cutting and skin-ablative properties of pulsed mid-infrared laser surgery. *J Dermatol Surg Oncol* **20**, 112–118 (1994).
3. Bekman H H P T, van den Heuvel J C, van Putten F J M, Schleijpen R. Development of a mid-infrared laser for study of infrared countermeasures techniques. *Proc. SPIE* **5615**, 27–38 (2004).
4. Zhu X S, Jain R. Watt-level 100-nm tunable 3-μm fiber laser. *IEEE Photonics Technol Lett* **20**, 156–158 (2008).
5. Li J F, Wang L L, Luo H Y, Xie J T, Liu Y. High power cascaded erbium doped fluoride fiber laser at room temperature. *IEEE Photonics Technol Lett* **28**, 673–676 (2016).
6. Aydin Y O, Fortin V, Vallée R, Bernier M. Towards power scaling of 2.8 μm fiber lasers. *Opt Lett* **43**, 4542–4545 (2018).
7. Jackson S D. Singly Ho^{3+}-doped fluoride fibre laser operating at 2.92 μm. *Electron Lett* **40**, 1400–1401 (2004).
8. Li J F, Luo H Y, Wang L L, Liu Y, Yan Z J et al. Mid-infrared passively switched pulsed dual wavelength Ho^{3+}-doped fluoride fiber laser at 3 μm and 2 μm. *Sci Rep* **5**, 10770 (2015).
9. Woodward R I, Hudson D D, Fuerbach A, Jackson S D. Generation of 70-fs pulses at 2.86 μm from a mid-infrared fiber laser. *Opt Lett* **42**, 4893–4896 (2017).
10. Jackson S D. Continuous wave 2.9 μm dysprosium-doped fluoride fiber laser. *Appl Phys Lett* **83**, 1316–1318 (2003).
11. Luo H Y, Li J F, Gao Y, Xu Y, Li X H et al. Tunable passively Q-switched Dy^{3+}-doped fiber laser from 2.71 to 3.08 μm using PbS nanoparticles. *Opt Lett* **44**, 2322–2325 (2019).
12. Coleman D J, King T A, Ko D K, Lee J. Q-switched operation of a 2.7 μm cladding-pumped Er^{3+}/Pr^{3+} codoped ZBLAN fibre laser. *Opt Commun* **236**, 379–385 (2004).
13. Hu T, Hudson D D, Jackson S D. Actively Q-switched 2.9 μm $Ho^{3+}Pr^{3+}$-doped fluoride fiber laser. *Opt Lett* **37**, 2145–2147 (2012).
14. Li J, Luo H, He Y L, Liu Y, Zhang L et al. Semiconductor saturable absorber mirror passively Q-switched 2.97 μm fluoride fiber laser. *Laser Phys Lett* **11**, 065102 (2014).
15. Frerichs C, Unrau U B. Passive Q-switching and mode-locking of erbium-doped fluoride fiber lasers at 2.7 μm. *Opt Fiber Technol* **2**, 358–366 (1996).
16. Wei C, Zhang H, Shi H, Konynenbelt K, Luo H et al. Over 5-W passively Q-switched mid-infrared fiber laser with a wide continuous wavelength tuning range. *IEEE Photonics Technol Lett* **29**, 881–884 (2017).
17. Li J F, Luo H Y, Wang L L, Zhao C J, Zhang H et al. 3-μm Mid-infrared pulse generation using topological insulator as the saturable absorber. *Opt Lett* **40**, 3659–3662 (2015).
18. Zhu G W, Zhu X S, Balakrishnan K, Norwood R A, Peyghambarian N. Fe^{2+}:ZnSe and graphene Q-switched singly Ho^{3+}-doped ZBLAN fiber lasers at 3 μm. *Opt Mater Exp* **3**, 1365–1377 (2013).
19. Li J F, Luo H Y, Zhai B, Lu R G, Guo Z N et al. Black phosphorus: a two-dimension saturable absorption material for mid-infrared Q-switched and mode-locked fiber lasers. *Sci Rep* **6**, 30361 (2016).
20. Zhu C H, Wang F Q, Meng Y F, Yuan X, Xiu F X et al. A robust and tuneable mid-infrared optical switch enabled by bulk Dirac fermions. *Nat Commun* **8**, 14111 (2017).
21. Dickinson B C, Golding P S, Pollnau M, King T A, Jackson S D. Investigation of a 791-nm pulsed-pumped 2.7-μm Er-doped ZBLAN fibre laser. *Opt Commun* **191**, 315–321 (2001).
22. Shen Y L, Huang K, Zhou S Q, Luan K P, Yu L et al. Gain-switched 2.8μm Er^{3+}-doped double-clad ZBLAN fiber laser. *Proc SPIE* **9543**, 95431E (2015).
23. Gorjan M, Petkovšek R, Marinček M, Čopič M. High-power pulsed diode-pumped Er:ZBLAN fiber laser. *Opt Lett* **36**, 1923–1925 (2011).
24. Li J F, Hu T, Jackson S D. Q-switched induced gain switching of a two-transition cascade laser. *Opt Express* **20**, 13123–13128 (2012).
25. Luo H Y, Li J F, Hai Y C, Lai X, Liu Y. State-switchable and wavelength-tunable gain-switched mid-infrared fiber laser in the wavelength region around 2.94 μm. *Opt Express* **26**, 63–79 (2018).
26. Jobin F, Fortin V, Maes F, Bernier M, Vallée R. Gain-switched fiber laser at 3.55 μm. *Opt Lett* **43**, 1770–1773 (2018).
27. Luo H Y, Li J F, Zhu C, Lai X, Hai Y C et al. Cascaded gain-switching in the mid-infrared region. *Sci Rep* **7**, 16891

(2017).
28. Luo H Y, Yang J, Liu F, Hu Z, Xu Y et al. Watt-level gain-switched fiber laser at 3.46 μm. *Opt Express* **27**, 1367–1375 (2019).
29. Shen Y L, Wang Y S, Luan K P, Chen H W, Tao M M et al. Efficient wavelength-tunable gain-switching and gain-switched mode-locking operation of a heavily Er^{3+}-doped ZBLAN mid-infrared fiber laser. *IEEE Photonics J* **9**, 1504510 (2017).
30. Wei C, Luo H Y, Shi H X, Lyu Y J, Zhang H et al. Widely wavelength tunable gain-switched Er^{3+}-doped ZBLAN fiber laser around 2.8 μm. *Opt Express* **25**, 8816–8827 (2017).
31. Shi Y, Li J, Luo H, Xu Y, Liu F et al. Gain-Switched Dual-Waveband Ho 3+ -Doped Fluoride Fiber Laser Based on Hybrid Pumping. *IEEE Photonic Techl* **31**, 46–49 (2019).
32. Paradis P, Fortin V, Aydin Y O, Vallée R, Bernier M. 10 W-level gain-switched all-fiber laser at 2.8 μm. *Opt Lett* **43**, 3196–3199 (2018).
33. Wetenkamp L, West G F, Többen H. Co-doping effects in erbium^{3+}-and holmium^{3+}-doped ZBLAN glasses. *J Non Cryst Solids* **140**, 25–30 (1992).
34. Yang J L, Tang Y L, Xu J Q. Development and applications of gain-switched fiber lasers [Invited]. *Photonics Res* **1** 52–57 (2013).
35. Dickinson B C, Jackson S D, King T A. 10 mJ total output from a gain-switched Tm-doped fibre laser. *Opt Commun* **182**, 199–203 (2000).
36. Le Flohic M, Franchois P L, Allain J Y, Sanchez F, Stephan G M. Dynamics of the transient buildup of emission in Nd^{3+}-doped fiber lasers. *IEEE J Quantum Electron* **27**, 1910–1921 (1991).
37. Jiang M, Tayebati P. Stable 10 ns, kilowatt peak-power pulse generation from a gain-switched Tm-doped fiber laser. *Opt Lett* **32**, 1797–1799 (2007).

Acknowledgements

This work is supported by National Natural Science Foundation of China (Nos. 61475129, 11674269), Fundamental Research Funds for the Central Universities (No. 20720180057); Natural Science Foundation of Fujian Province for Distinguished Young Scientists (No. 2017J06016); Dr. Luo is grateful for supports from the Program for the Young Top Notch Talents of Fujian Province and the Program for the Nanqiang Young Top Notch Talents of Xiamen University.

Competing interests

The authors declare no competing financial interests.